Supplement of Clim. Past, 17, 1119–1138, 2021
https://doi.org/10.5194/cp-17-1119-2021-supplement

Climate of the Past
Open Access
EGU

Supplement of

A data–model approach to interpreting speleothem oxygen isotope records from monsoon regions

Sarah E. Parker et al.

Correspondence to: Sarah E. Parker (s.parker@pgr.reading.ac.uk)

Figure S1: ECHAM5-wiso annual precipitation-weighted mean $\delta^{18}O_{precip}$ anomalies for the mid-Holocene period (MH, 6,000 years BP, SMOW, ‰) and SISAL $\delta^{18}O_{spel}$ MH anomalies (6,000 years BP ± 500 years, PDB, ‰) , plotted as positive or negative signals with respect to 1850-1990 CE. 54 sites have isotope samples in the base period and the MH, 72% of sites show changes in the same direction as ECHAM MH $\delta^{18}O_{precip}$ anomalies, allowing for an uncertainty of ±0.5 ‰.

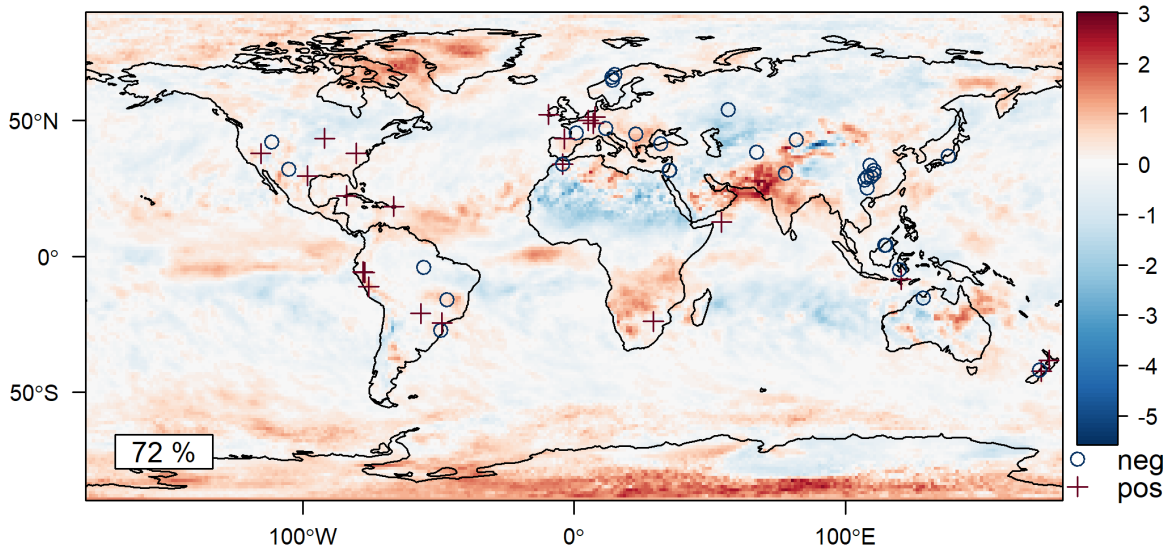

Figure S2: ECHAM5-wiso annual precipitation-weighted mean $\delta^{18}O_{precip}$ anomalies for the LGM (21,000 years BP, SMOW, ‰) and SISAL $\delta^{18}O_{spel}$ LGM anomalies (21,000 years BP ± 1,000 years, PDB, ‰), plotted as positive or negative signals with respect to 1850-1990 CE. 17 sites have isotope samples in the base period and the LGM. 76% of sites show changes in the same direction as ECHAM LGM $\delta^{18}O_{precip}$ anomalies, allowing for an uncertainty of ±0.5 ‰.

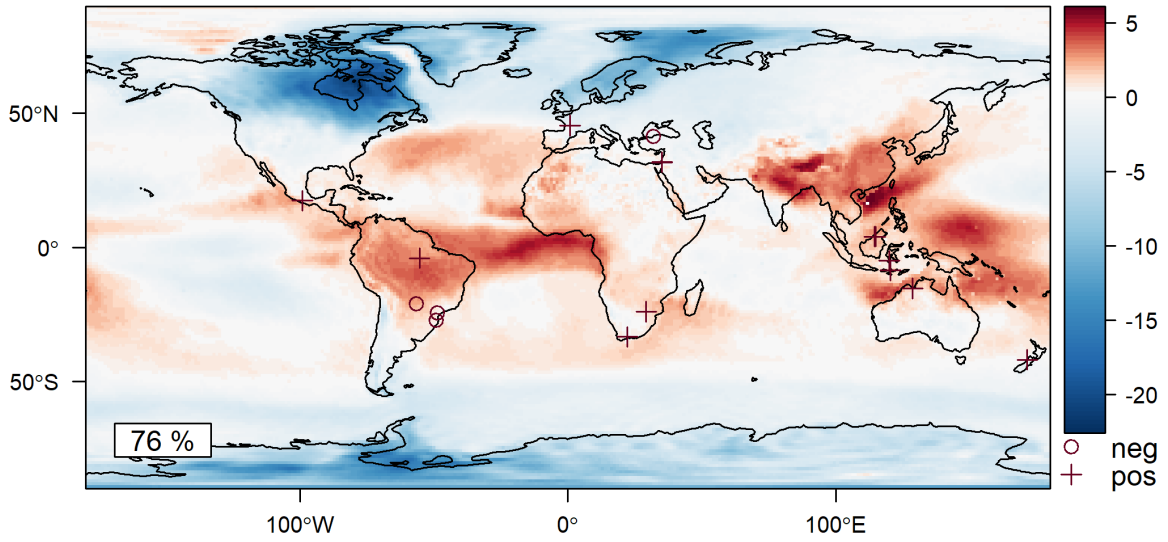

Figure S3: ECHAM5-wiso annual precipitation-weighted mean $\delta^{18}O_{precip}$ anomalies (SMOW, ‰) for the LIG (125,000 years BP) and SISAL $\delta^{18}O_{spel}$ LIG anomalies (125,000 years BP ± 1,000 years, PDB, ‰), plotted as positive and negative signals with respect to 1850-1990 CE. 12 sites have isotope samples in the base period and the LIG. All sites show changes in the same direction as ECHAM LIG $\delta^{18}O_{precip}$ anomalies, allowing for an uncertainty of ±0.5 ‰.

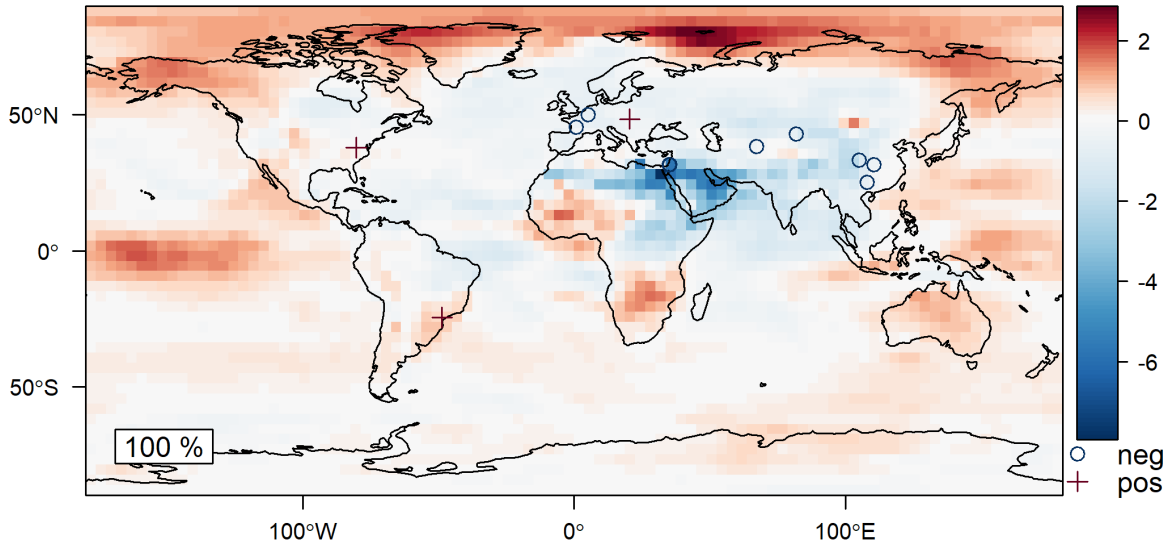

Figure S4: GISS annual precipitation-weighted mean $\delta^{18}O_{precip}$ anomalies for 3,000 years BP (3ka, SMOW, ‰) and SISAL $\delta^{18}O_{spel}$ 3ka anomalies (3,000 years BP ± 500 years, PDB, ‰), plotted as positive and negative signals with respect to 1850 to 1990 CE. 63 sites have isotope values in the

base period and 3ka. 87% show changes in the same direction as GISS $\delta^{18}O_{precip}$ 3ka anomalies, allowing for an uncertainty of ±0.5 ‰.

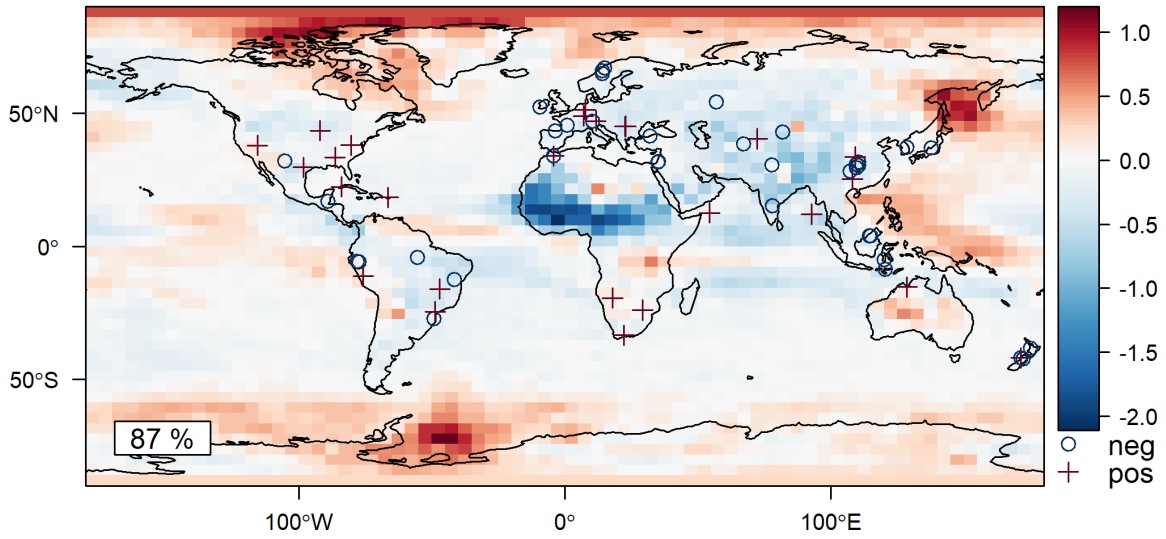

Figure S5: GISS annual precipitation-weighted mean $\delta^{18}O_{precip}$ anomalies for 6,000 years BP (6ka, SMOW, ‰) and SISAL $\delta^{18}O_{spel}$ 6ka anomalies (6,000 years BP ± 500 years, PDB, ‰), plotted as positive and negative signals with respect to 1850 to 1990 CE. 54 sites have isotope values in the base period and 6ka. 87% show changes in the same direction as GISS $\delta^{18}O_{precip}$ 3ka anomalies, allowing for an uncertainty of ±0.5 ‰.

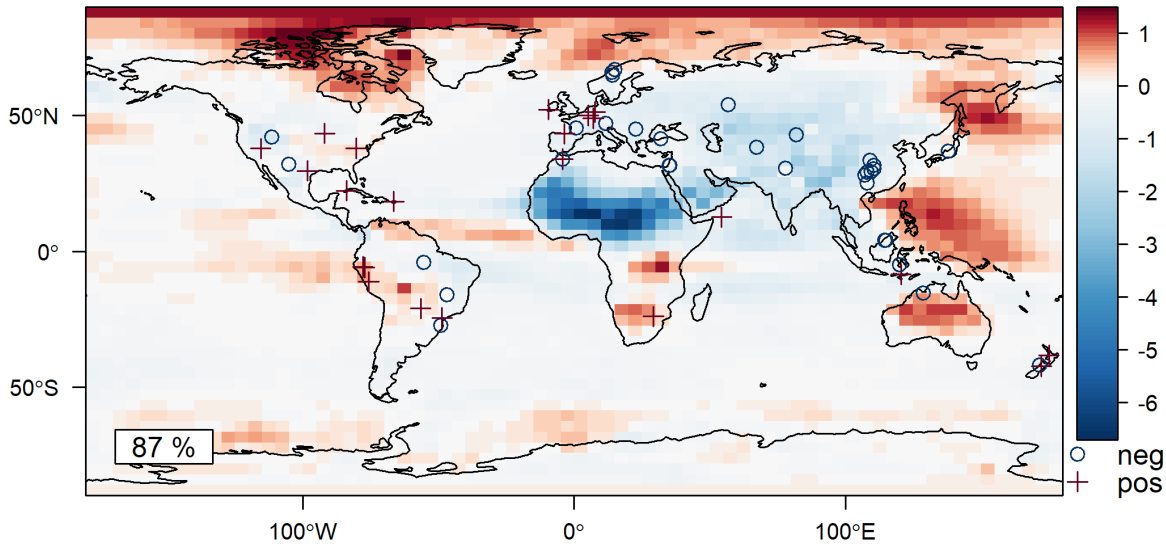

Figure S6: GISS annual precipitation-weighted mean $\delta^{18}O_{precip}$ anomalies for 9,000 years BP (9ka, SMOW, ‰) and SISAL $\delta^{18}O_{spel}$ 9ka anomalies (9,000 years BP ± 500 years, PDB, ‰), plotted as positive and negative signals with respect to 1850 to 1990 CE. 48 sites have isotope values in the base period and 9ka. 81% show changes in the same direction as GISS $\delta^{18}O_{precip}$ 9ka anomalies, allowing for an uncertainty of ±0.5 ‰.

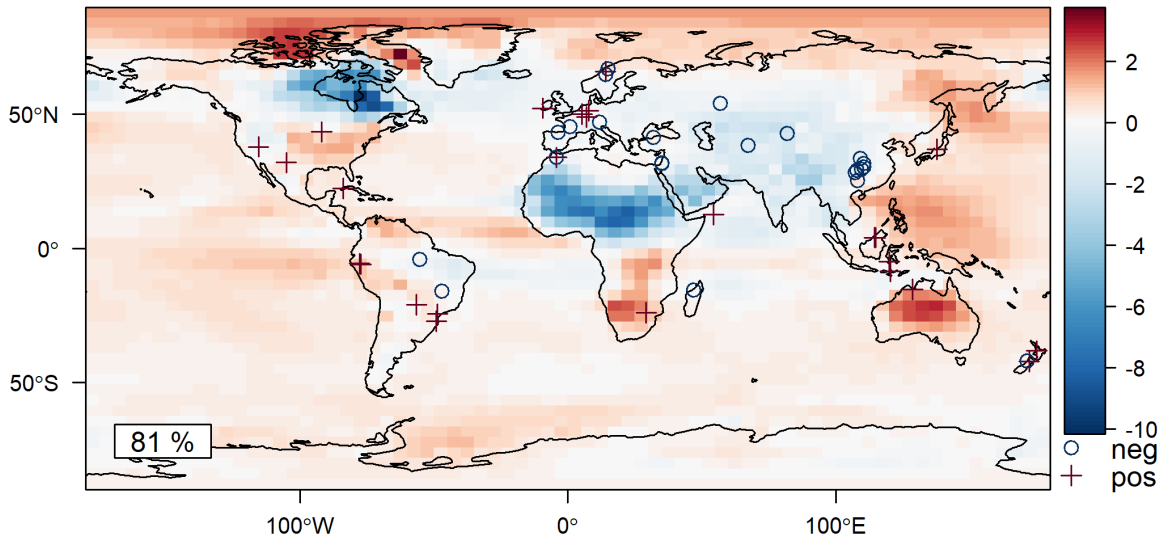

Figure S7: Spatial distribution of speleothem sites used in this study, shown with monsoon regions, defined by the precipitation-based criteria (Wang and Ding, 2008): the annual precipitation range (summer minus winter) exceeds 300 mm and 50 % of the annual mean. Summer is defined as May to September for the northern hemisphere and November to March for the southern hemisphere, vice versa for winter. Precipitation data is from the WFDEI dataset (Weedon et al., 2014).

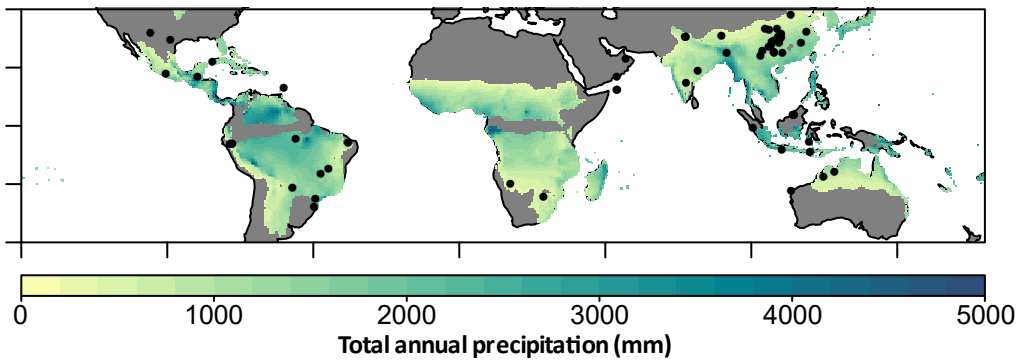

Figure S8: Speleothem $\delta^{18}O$ anomalies, converted to their drip water equivalent, compared to anomalies of $\delta^{18}O_{precip}$ from the ECHAM simulations for the (a) East Asian (EAM), (b) Indian (ISM) and (c) Indonesian-Australian (IAM) monsoons. $\delta^{18}O_{spel}$ (PBD) is converted to $\delta^{18}O_{drip\ water}$ (SMOW) following the methodology in Comas-Bru et al. (2019), using simulated temperature. The boxes show the median value (line) and the interquartile range, and the whiskers shown the minimum and

maximum values, with outliers represented by grey dots. Note that the isotope axes are reversed, so that the most negative anomalies are at the top of the plot, to be consistent with the assumed relationship with the direction of change in precipitation and temperature. The difference in amplitude of $\delta^{18}O$ signals is small (<0.5 ‰) between simulated and observed values for the ISM and IAM. In the EAM, simulated $\delta^{18}O$ values have a ~1.4 ‰ higher amplitude than $\delta^{18}O_{drip\ water}$ observations.

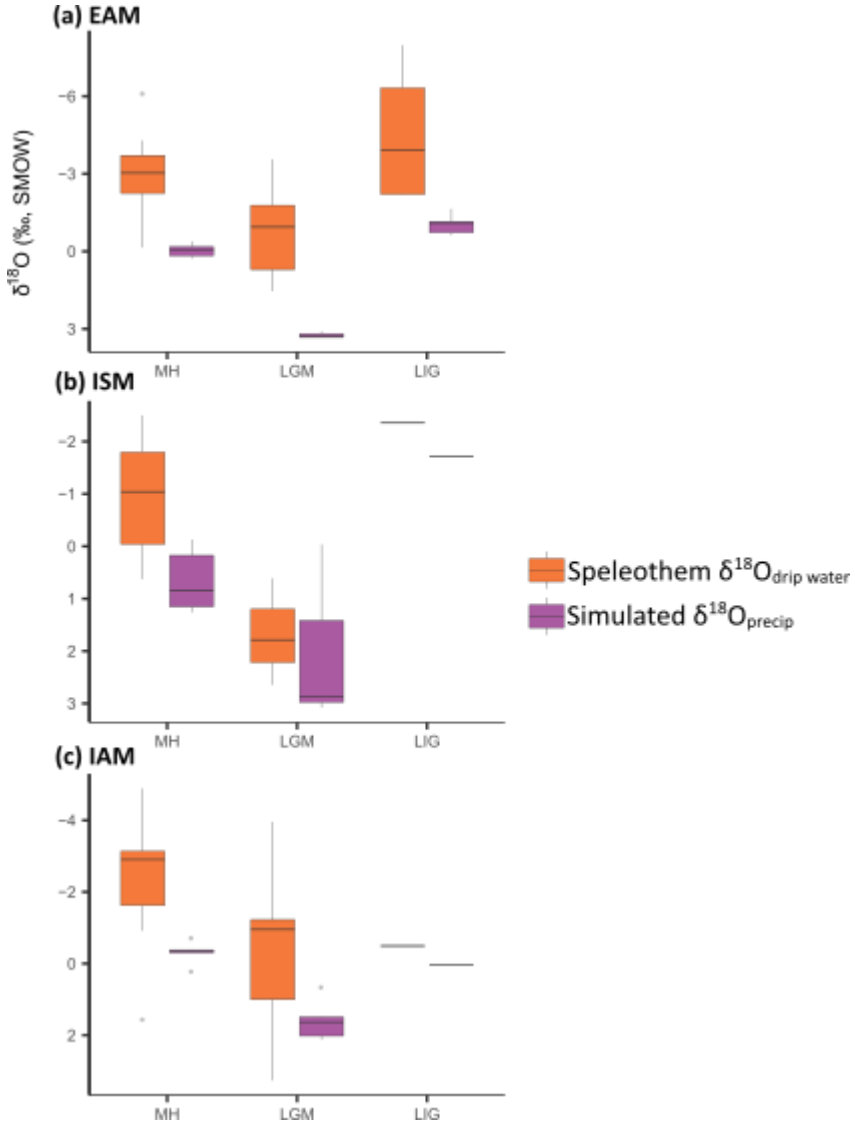

Figure S9: Same as figure 6, except Indian Summer Monsoon (ISM) source region has been expanded to include the Bay of Bengal.

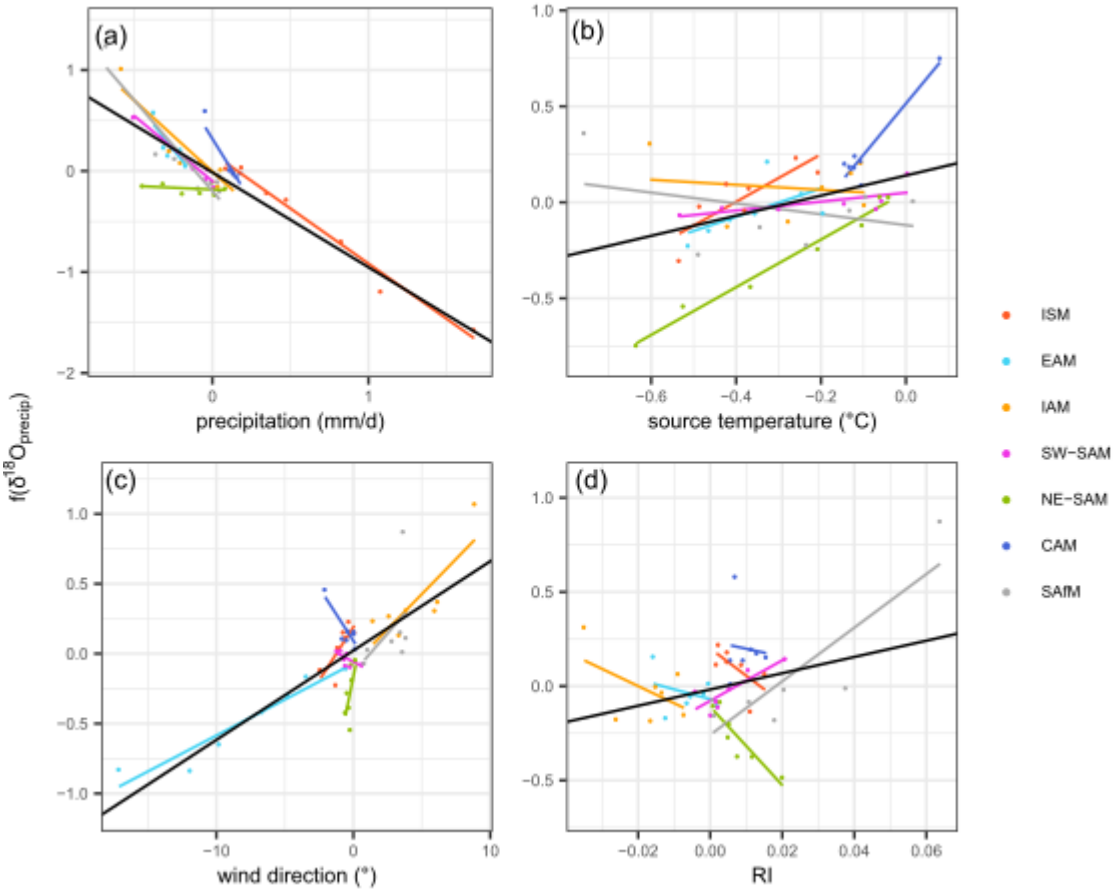

Table S1: Results of the multiple linear regression analysis when the Indian monsoon source region is expanded to include the Bay of Bengal. Significant relationships (P > 0.01) are shown in bold.

	Regression coefficient	T value
Regional precipitation	**-0.94**	-11.22
Source area temperature	**0.52**	2.95
Wind direction	**0.06**	8.30
Precipitation recycling	4.32	1.95

Comas-Bru, L., Harrison, S. P., Werner, M., Rehfield, K., Scroxton, N., Veiga-Pires, C. and SISAL working group members: Evaluating model outputs using integrated global speleothem records of climate change since the last glacial, Clim. Past, 15(4), 1557–1579, https://doi.org/10.5194/cp-15-1557-2019, 2019.

Wang, B. and Ding, Q.: Global monsoon: Dominant mode of annual variation in the tropics, Dyn. Atmos. Ocean., 44(3–4), 165–183, https://doi.org/10.1016/j.dynatmoce.2007.05.002, 2008.

Weedon, G. P., Balsamo, G., Bellouin, N., Gomes, S., Best, M. J. and Viterbo, P.: The WFDEI meteorological forcing data set: WATCH Forcing Data methodology applied to ERA-Interim reanalysis data, Water Resour. Res., 50(9), 7505–7514, https://doi.org/10.1002/2014WR015638, 2014.